

# Evaluation of the physico-mechanical and electrical properties of styrene-butadiene rubber/aluminum powder and styrene-butadiene rubber/cerium sulfate composites

Amira Nassar<sup>1), \*), A.A. Yehia<sup>2)</sup>, S.H. El-Sabbagh<sup>2)</sup></sup>

DOI: dx.doi.org/10.14314/polimery.2015.100

**Abstract:** Different concentrations of powdered aluminum (Al) or cerium sulfate in the range between 10 and 60 phr were incorporated into styrene-butadiene rubber (SBR) matrices. The physico-mechanical and electrical properties of vulcanizates were measured and evaluated. An improvement in the mechanical properties according to increased filler loading in SBR composites was noted. This finding is reinforced by filler dispersion values (Lee equation), reinforcing index and thermal analysis.

The dielectric properties, namely the relative permittivity ( $\epsilon'$ ) and dielectric loss ( $\epsilon''$ ), were measured as function of both frequency and concentration of the SBR/filler composites. The results showed an enhancement in the dielectric and mechanical properties, especially for Al powder. This is due to the enhancement of filler-rubber interactions and the continuity of the conductive phase through the composites. The SEM micrograph showed that the filler agglomerates were dispersed within the SBR matrix.

**Keywords:** aluminum powder, cerium sulfate, styrene-butadiene rubber, mechanical properties, image analysis, electrical properties.

## Ocena fizyko-mechanicznych i elektrycznych właściwości kauczuku butadienowo-styrenowego napełnionego proszkami aluminium lub siarczanu(VI) ceru(IV)

**Streszczenie:** Do matrycy kauczuku butadienowo-styrenowego (SBR) wprowadzano proszki aluminium (Al) lub siarczanu(VI) ceru(IV) w ilości 10–60 phr. Oceniono właściwości fizyko-mechaniczne i elektryczne wytworzonych wulkanizatów. Stwierdzono, że wraz ze zwiększeniem zawartości cząstek napełniacza w matrycy SBR poprawiały się właściwości mechaniczne kompozytów, co potwierdzono metodą analizy termograwimetrycznej, na podstawie indeksu wzmacniania ( $RI$ ) oraz stopnia dyspersji napełniacza. Badano też zależność właściwości dielektrycznych – względnej przenikalności ( $\epsilon'$ ) i strat dielektrycznych ( $\epsilon''$ ) – od częstotliwości zewnętrznego pola magnetycznego i od stężenia cząstek napełniacza w matrycy SBR. Wyniki wskazują na polepszenie właściwości zarówno dielektrycznych, jak i mechanicznych zwłaszcza w przypadku kauczuku napełnionego proszkiem aluminium. Obserwowaną poprawę przypisano interakcjom między cząstkami napełniacza i kauczuku, skutkującym przewodnością fazy ciągłej kompozytów. Mikrofotografie SEM wskazują na obecność aglomeratów cząstek napełniacza rozproszonych w matrycy kauczuku SBR.

**Słowa kluczowe:** aluminium w postaci proszku, siarczan(VI) ceru(IV), kauczuk butadienowo-styrenowy, właściwości mechaniczne, właściwości elektryczne.

Industrial activities reveal a continuous demand for improved materials that satisfies increasingly stringent requirements such as high physico-mechanical characteristics with cost reduction. These requirements can be achieved through the use of composite materials whose constituents synergistically comply with the needs for

specific applications [1]. In most industrial applications, elastomers are used as a matrix for very fine particulates for the production of composite materials. Such particles can interact physically and/or chemically with the elastomers creating high performance polymeric composites [2]. Metallic powders are a special type of particle filler that impart special qualities to rubber composites. These fillers enhance properties such as thermal conductivity, electrical conductivity, response to magnetic fields, heat capacity, etc. Polymeric, metal-filled composites are used as antistatic materials in tires and wind blades to dissipate the accumulated electrostatic charges [3].

<sup>1)</sup> National Research Centre, Solid State Physics Department, Metal Physics Laboratory, Dokki, Giza, Egypt.

<sup>2)</sup> National Research Centre, Polymers and Pigments Department, Dokki, Cairo, Egypt.

<sup>\*</sup> Author for correspondence; e-mail: fatmohmar@yahoo.com

The incorporation of metal fillers not only improves the electrical properties of the rubbers but also enhances the thermal conductivity of the rubber composites [4]. Studies on the performance of rubber-metal pairs have been an important area in the tribology research field. There are many interrelated reports on determining the way to decrease the friction coefficient and improve the mechanical properties of rubber composites [5]. Various methods are available to increase the conductivity of rubbers. One of the best and easily applied methods is the incorporation of metal powders. Poor adhesion and non-uniform dispersion of the discrete phase in the matrix cause fluctuations in the composite properties. This can be overcome by using coupling/bonding agents, which increase the rubber-filler interactions [6].

The application of rare earth salts in rubber is a new research area. Related studies showed that rare earth compounds had a particular function in rubber processing and application, such as heat stability, strengthening action, etc. Cerium sulfate and cerium oxide are considered the most important rare earth compounds. They are extensively applied in glass, ceramics, catalysis, polishing powders, phosphor, absorption ultraviolet material, etc. [3, 7].

The aim of the present work is to evaluate the effect of powdered aluminum (Al) and cerium sulfate  $[Ce(SO_4)_2]$  as reinforcing fillers for a styrene-butadiene rubber (SBR) matrix through the measurement of the mechanical, rheological, scanning electron microscope (SEM) and dielectric properties. A secondary aim is to study the effect of different loadings (10–60 phr) of the investigated fillers on the properties of SBR.

## EXPERIMENTAL PART

### Materials

— SBR, is a styrene-butadiene rubber (1502) with 23.5 % styrene content, a molecular weight  $M_W$  of 140 000 g/mole, Mooney viscosity  $ML(1 + 4)$  at 100 °C =  $52 \pm 3$ , and glass transition  $T_g = -60$  °C. Supply is Kumho, LG, Zeon, ENI, and Sinopec CQ. Made in China.com connecting Buyers with china suppliers. Trade terms: FOB.

— Fine aluminum (Al) powder, particle size in the range 1.74–2.12 µm, 99 % trace grade of metals basis, molecular weight 26.97 g/mol, boiling point 2327 °C, flash point 645 °C and density 2.7 g/cm<sup>3</sup>, was supplied by Aldrich (USA 18530. 1M). The chemical composition of Al powder is presented in Table 1.

— Cerium(IV) sulfate  $Ce(SO_4)_2$  powder, oxydimetric min. 98 %, particle size in the range 4.88–13.9 µm was supplied by E. Merck, Darmstadt, Germany.

— Accelerators: *N*-cyclohexyl-2-benzothiazole sulfenamide (CBS), trade name: Rhenogran® CBS-80, Vulcacit® CZ. From Rheinehemie Germany.

— Antioxidants TMQ — polymerized 2,2,4-trimethyl-1,2-dihydroquinoline, trade name: PILnox® TDQ.

**Table 1. Chemical composition of aluminum powder**

Component	Concentration, ppm
Iron (Fe)	≤ 3500
Silicon (Si)	≤ 2500
Copper (Cu)	≤ 200
Zinc (Zn)	≤ 500
Titanium (Ti)	≤ 200

From NOCIL LIMITED Navi Mumbai, Maharashtra 400705, India.

— Activators: stearic acid with density at 15 °C of 0.9–0.97 g/cm<sup>3</sup>, zinc oxide (ZnO) with density at 15 °C of 5.55–5.61 g/cm<sup>3</sup>, were supplied by Aldrich Company, Germany.

— Curing agent: elemental sulfur as vulcanizing agent with fine pale yellow powder and density of 2.04–2.06 g/cm<sup>3</sup> at room temperature ( $25^{\circ}C \pm 1$ ) was supplied by Aldrich Company, Germany.

The above-mentioned ingredients are generally used in the rubber industry. The solvents and chemicals were of pure grade.

### Sample preparation

Different concentrations of aluminum (Al) or cerium sulfate  $[Ce(SO_4)_2]$  powder at 10, 20, 30, 40, 50 or 60 phr were mixed with SBR and the other ingredients according to ASTM D 15-72 (2007) in a two-roll mill. The speed of the slow roller was 24 rpm and the gear ratio was 1:1.4. Vulcanization was carried out in a single-daylight, electrically heated, auto controlled by hydraulic press at 152 °C under a pressure of 4 MPa at the curing time, which was determined by an oscillating disc rheometer. The compounded rubber and vulcanizates were tested according to standard methods.

The specimens were made into disks of diameter 10 mm and thickness 2 mm for the electrical measurements.

### Methods of testing

— The mechanical properties were determined according to ASTM D 412-06a (2013) and ASTM D 6204-12 (2012). The rheometric characteristics were measured at 152 °C using a Monsanto Rheometer (model 100) according to ASTM D 2084-11, hardness was determined according to ASTM 2240-07 (2007) and swelling was determined according to ASTM D 3616-95 (2009).

The swelling data were utilized to determine the molecular weight between two successive crosslinks ( $M_c$ ) through the Flory-Rehner relationship [7]:

$$\frac{1}{2M_c} = -\frac{1}{2\rho V_0} \left[ \ln(1-V_r) + V_r + \mu V_r^2 \right] / \left( V_r^{1/3} - \frac{1}{2} V_r \right) \quad (1)$$

where:  $\rho$  — the density of rubber,  $V_0$  — the molar volume of solvent (toluene),  $V_r$  — the volume fraction of the swollen rubber, and  $\mu$  — the interaction parameter between the rubber and toluene (0.446) [8].

The cross linking density ( $N$ ) can be calculated from the equation:

$$N = (1/2 M_c) \quad (2)$$

— Scanning electron microscopy (SEM) — Phase morphology was studied using a JEOL JXA-840A electron probe micro analyzer supplied by JEOL, Japan. The fracture surfaces were gold coated to avoid electrostatic charging during examination.

— Electric properties — The dielectric properties of the specimens were measured using a Schlumberger Solartron (1260) in the frequency ( $f$ ) range from  $f = 10^{-1}$  Hz to  $f = 5 \cdot 10^6$  Hz, at room temperature 30 °C.

— Thermogravimetric analysis (TGA) of the composites was carried out using Perkin Elmer analyzer equipment, USA. Sample weights between 13 and 32 mg were scanned from 50 to 1000 °C using a nitrogen air flow of 50 cm<sup>3</sup>/min and a heating rate of 10 °C/min.

## RESULTS AND DISCUSSION

### Morphology of SBR/powder composites

Conventional SEM is used to study the surface morphologies of the prepared composites. The SEM micrographs are shown in Fig. 1. It was observed that the SEM microphotograph of SBR without fillers revealed a good

distribution of rubber ingredients such as zinc oxide and curative sulfur in the SBR matrix, as shown in (Fig. 1a). The SEM micrographs for SBR/Al composites loaded with 10 and 60 phr are shown in Fig. 1b and 1c. A uniform distribution of Al powder was observed in the continuous SBR phase. It is worth noting the agglomeration of the Al particles as a function of increased concentration. The SEM micrographs for the composite of SBR/cerium sulfate [SBR/Ce(SO<sub>4</sub>)<sub>2</sub>] composites loaded with 10 and 60 phr of cerium sulfate powder are shown in (Fig. 1d, e); one can clearly see the intense agglomeration of cerium sulfate powder. Also, the boundaries between cerium sulfate particles and SBR matrix are clearly seen. This may explain the low mechanical properties of such composites described below.

### Rheological properties

The determined rheological properties of SBR/Al and SBR/Ce(SO<sub>4</sub>)<sub>2</sub> composites are given in Table 2. It can be deduced that the incorporation of such fillers in the SBR matrix increased the  $M_H$  and  $M_L$  values, as well as  $\Delta M$  values up to 50 phr for Al and 40 phr for Ce(SO<sub>4</sub>)<sub>2</sub>, before decreasing. The decrease of torque value at high loading of the investigated fillers may be attributed to a reaction between the aluminum (Al) or cerium sulfate with the curative, which translates into a small increase in the cross-link density and decrease in torque. On the other hand, the increment of torque values can be attributed to a physical interaction between SBR and filler phase surfaces and the hydrodynamic effect [9–11]. The maximum tor-

**T a b l e 2. Formulation, rheometric characteristics and filler dispersion parameters of SBR/filler composites at 152 °C**

Filler content, phr	$M_L$ , dNm	$M_H$ , dNm	$t_{C90}$ , min	$t_{S2}$ , min	CRI, min <sup>-1</sup>	$\Delta M$ , dNm	$\alpha_f$	$\eta_r$	$M_r$	$L$
Aluminum powder										
0	7.0	41.0	17.5	7.75	10.25	34.0	-	-	-	-
10	7.5	43.0	17.0	7.75	10.81	35.5	0.441	1.07	1.05	0.02
20	8.0	45.0	13.0	7.00	16.67	37.0	0.441	1.14	1.09	0.05
30	8.5	46.0	12.0	7.13	20.51	37.5	0.343	1.21	1.12	0.09
40	8.8	47.3	11.8	6.19	17.98	38.5	0.331	1.25	1.15	0.10
50	9.0	48.5	11.5	5.00	15.38	39.5	0.324	1.28	1.18	0.10
60	8.8	43.0	13.5	6.88	15.11	34.3	0.012	1.25	1.05	0.20
Cerium sulfate powder										
10	4.0	47.8	8.4	3.00	18.60	43.8	15.735	1.14	2.33	- 1.19
20	5.0	40.5	11.3	3.00	12.12	35.5	5.441	1.43	1.98	- 0.55
30	5.5	40.5	12.8	2.38	9.64	35.0	3.529	1.57	1.98	- 0.41
40	5.3	31.0	15.3	3.63	8.60	25.8	0.367	1.50	1.22	0.28
50	5.0	23.5	17.0	4.00	7.70	18.5	0.176	1.43	1.15	0.28
60	4.5	22.5	18.0	4.50	7.41	18.0	0.024	1.36	1.10	0.26

Base recipe (in phr): SBR — 100; stearic acid — 2; zinc oxide — 5; CBS (*N*-cyclohexyl-2-benzothiazole sulfenamide) — 0.8; TMQ — polymerized 2,2,4-trimethyl-1,2-dihydroquinoline — 1; sulfur — 2;  $\Delta M$  — the difference between maximum torque  $M_H$  and minimum torque  $M_L$ ;  $t_{S2}$  — scorch time;  $t_{C90}$  — optimum cure time; CRI — cure rate index,  $\alpha_f$  — specific constants for the fillers;  $\eta_r$  — the relative viscosity;  $M_r$  — the relative modulus,  $L = \eta_r - M_r$ , where phr is part per hundred parts of rubber.

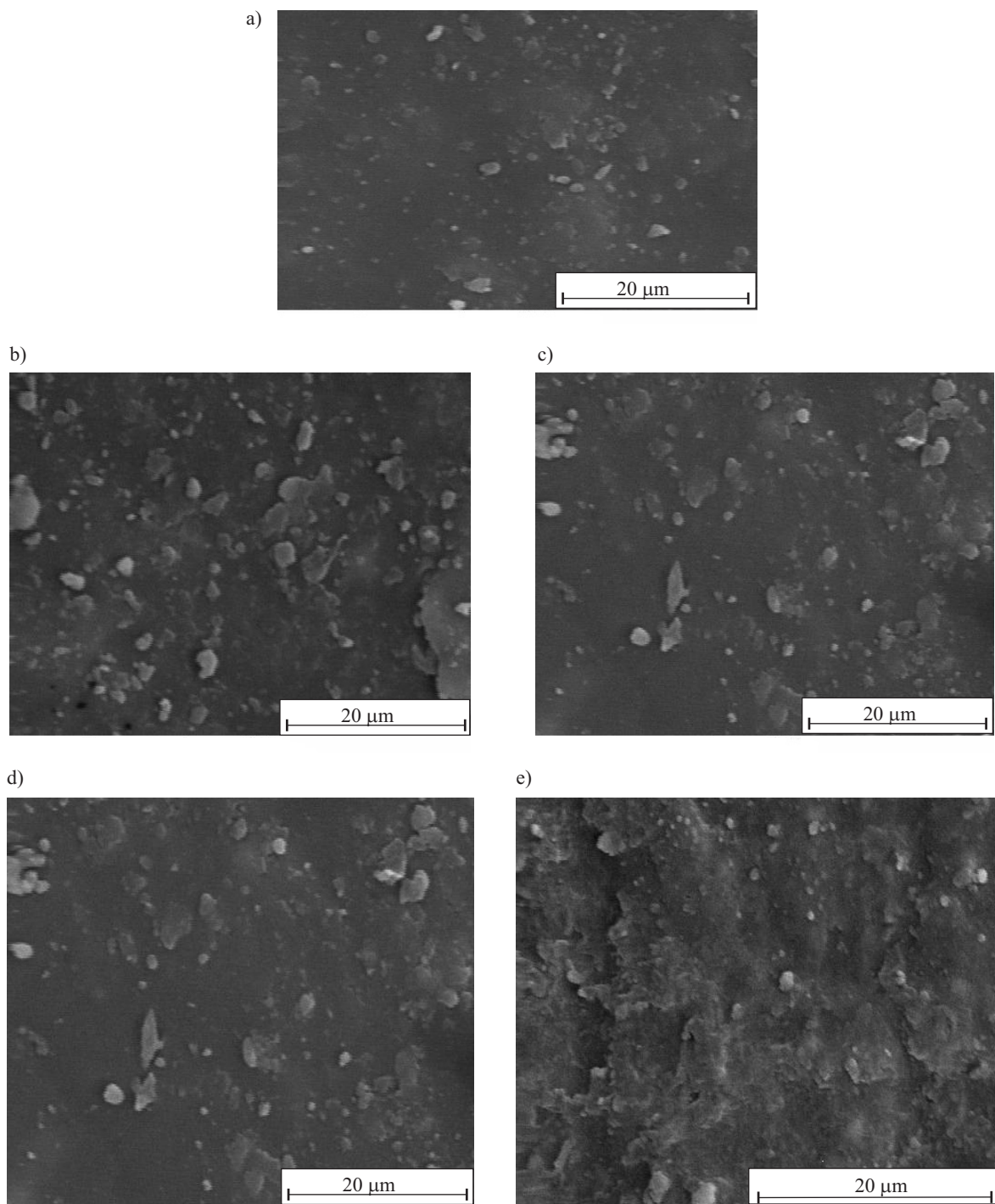


**Fig. 1.** SEM images of: a) SBR without filler, b) SBR/10 phr Al, c) SBR/60 phr Al, d) SBR/10 phr  $\text{Ce}(\text{SO}_4)_2$ , e) SBR/60 phr  $\text{Ce}(\text{SO}_4)_2$  composites at magnification 2000 $\times$

que  $M_H$  can be regarded as a measure of the composites' modulus [4], while the minimum torque ( $M_L$ ) is an indirect measure of the viscosity of the rubber composites [10, 12]. Therefore, the incorporation of Al or  $\text{Ce}(\text{SO}_4)_2$  powder into the SBR matrix increased the  $M_L$  values and, consequently, the viscosity of the composites as shown in Table 2. This can be due to the fact that the filler tends to impose extra resistance to the flow of the mixes [13]. The  $\Delta M$  values show a similar trend since  $\Delta M$  can be considered a measure of the dynamic shear modulus, which was

ascribed to the cross linking of the rubber phase [14]. The increment of  $\Delta M$  values may be due to the additional physical cross links created in the rubber matrix. This can be proved by equilibrium swelling ( $Q$ ) data and the calculated cross linking density ( $N$ ), which is given in Table 3.

On the other hand, the presence of aluminum particles in the SBR matrix has accelerated the curing process as shown in (Table 2), *i.e.* decreased the scorch time ( $t_{\text{s}2}$ ) and optimum cure time ( $t_{C90}$ ), up to 50 phr of Al and then

Table 3. Physico-mechanical properties of the SBR/filler composites

Property \ Al content, phr	0	10	20	30	40	50	60
<i>S<sub>e</sub></i> <sub>100</sub> , MPa	0.81±0.01	1.43±0.01	1.49±0.05	1.55±0.02	1.68±0.01	1.58±0.01	1.49±0.04
<i>TS<sub>b</sub></i> , MPa	1.98±0.17	3.64±0.04	3.95±0.07	4.04±0.09	4.55±0.06	5.78±0.06	4.39±0.09
<i>E<sub>b</sub></i> , %	385±3	372±2	360±2	345±2	339±2	334±2	324±2
<i>H</i> , Sh A	40±1.03	44±1.05	49±1.01	51±1.03	53±1.08	56±1.06	57±1.06
<i>Q<sub>m</sub></i> in toluene, %	359±0.4	321±0.1	316±1.0	312±1.1	312±1.0	309±1.0	299±0.9
<i>N</i> · 10 <sup>5</sup> , mole/cm <sup>3</sup>	6.8±0.8	8.5±0.3	8.7±0.1	8.9±0.4	8.9±0.3	9.1±0.6	9.7±0.2
<i>M<sub>C</sub></i> , g/mol	7396±1	5916±2	5735±2	5591±1	5591±2	5484±2	5138±3
Property \ Ce(SO <sub>4</sub> ) <sub>2</sub> content, phr	0	10	20	30	40	50	60
<i>S<sub>e</sub></i> <sub>100</sub> , MPa	0.81±0.01	0.92±0.02	1.18±0.01	1.29±0.01	1.34±0.01	1.15±0.05	1.15±0.03
<i>TS<sub>b</sub></i> , MPa	1.98±0.17	1.56±0.06	2.72±0.01	2.92±0.009	4.02±0.12	3.96±0.05	3.16±0.04
<i>E<sub>b</sub></i> , %	385±3	114±1	224±1	226±2	227±2	225±2	220±2
<i>H</i> , Sh A	40±1.0	39±0.2	44±0.1	46±0.3	50±0.4	51±0.2	51±0.1
<i>Q<sub>m</sub></i> in toluene, %	359±0.4	234±0.6	227±0.8	225±0.7	202±0.3	259±0.5	259±1.1
<i>N</i> · 10 <sup>5</sup> , mol/cm <sup>3</sup>	6.8±0.8	15.8±0.5	16.7±0.4	17.0±0.2	20.9±0.4	12.9±0.1	12.9±0.6
<i>M<sub>C</sub></i> , g/mol	7396±1	3173±1	2991±1	2940±1	2389±1	3869±1	3869±1

increased. This may be due to the chemical amphoteric nature of Al. The presence of cerium sulfate particles in the composite increased the optimum cure time (*t<sub>C90</sub>*) and consequently decreased the cure rate. This increase may be due to the acidic nature of cerium sulfate [3] (as shown in Table 2).

### Filler dispersion

The filler dispersion and formation of filler agglomerates in polymer matrices have been studied by Lee [15]. Lee assumed that the relative viscosity ( $\eta_r$ ) and the relative modulus ( $M_r$ ) could be determined from rheometric data through the expressions:

$$\eta_r = \frac{M_L^f}{M_L^0} \quad M_r = \frac{M_H^f}{M_H^0} \quad (3)$$

where:  $M_H$ ,  $M_L$  — denotes the torque maximum and minimum, respectively, and the superscripts, *f* and 0 — related to the loaded and the unloaded polymer, respectively. Also, Lee introduced a parameter *L*, defined as:

$$L = \eta_r - M_r \quad (4)$$

The torque variation for the loaded and unloaded composites is directly proportional to filler loading, a straight line is obtained, its' slope was defined by Wolf as  $\alpha_f$  [16, 17].

$$\left[ \frac{M_H^f - M_L^f}{M_H^0 - M_L^0} \right] - 1 = \alpha_f \left( \frac{m_f}{m_p} \right) \quad (5)$$

where:  $m_p$  — the mass of polymer in the composites,  $m_f$  — the mass of filler in the same composites and  $\alpha_f$  — is a specific constant for the filler, which is independent of the

cure system and closely related to the morphology of the filler. Also,  $\alpha_f$  can be calculated from the changes in the torque, which occur during vulcanization of the two compounds, the loaded and unloaded one (Fig. 2).

Table 2 shows the computed  $\eta_r$ ,  $M_r$  and *L* values of SBR/Al and SBR/Ce(SO<sub>4</sub>)<sub>2</sub> composites. One can see that in the case of filled SBR composites with aluminum (Al), the filler particles are well dispersed in the matrix except at higher loadings. Both  $\eta_r$  and  $M_r$  values increased with aluminum loading, indicating an increase in the relative viscosity and relative modulus of the elastomer except at 60 phr of Al loading, where the values of  $\eta_r$  or  $M_r$  decreased [14].

In SBR/cerium sulfate composites, there is a large difference between  $\eta_r$  and  $M_r$  values, since for 10, 20 and

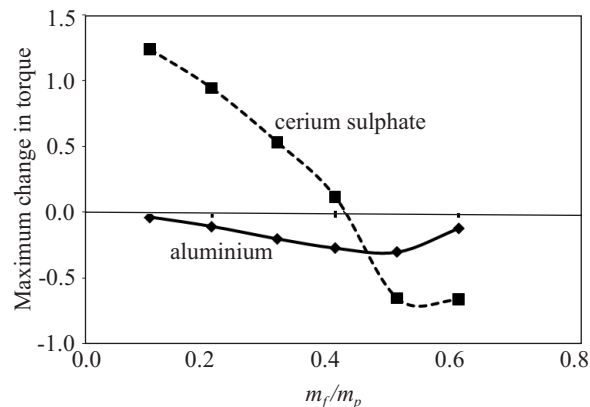


Fig. 2. Maximum changes in cure meter torque during vulcanization as a function of mass of investigated filler/mass of polymer ( $m_f/m_p$ )

30 phr the values of  $\eta_r$  is less than that of  $M_r$ . This may be due to agglomeration of the filler in the elastomer and this is in good agreement with the SEM data. On the other hand,  $\alpha_f$  values of SBR/filler composites are found to decrease with filler loading. This indicates that the investigated filler particles are well dispersed in the SBR matrix [15].

### Mechanical properties

The mechanical properties, namely: stress at 100 % elongation ( $S_{e100}$ ), tensile strength ( $TS_b$ ), elongation at break ( $E_b$ ) and hardness ( $H$ ) of SBR/Al and SBR/Ce(SO<sub>4</sub>)<sub>2</sub> composites versus filler content are given in (Table 3). It is clear from these data that the mechanical properties improve with increasing of filler content up to 50 phr Al and 40 phr Ce(SO<sub>4</sub>)<sub>2</sub>. This can be related to the interfacial adhesion and physical bonding between the filler and SBR matrix. These interactions facilitate the stress-transfer from the SBR matrix to the fillers under investigation. A further increase in filler content deteriorates the mechanical properties of the composites. The decrease in elongation and swelling is the typical characteristic for inorganic filled composites [18].

On the other hand, hardness, which depends on the distribution of the rigid filler in the SBR matrix, is increased with higher contents of Al or Ce(SO<sub>4</sub>)<sub>2</sub>. It is well known that incorporation of the filler particles in the soft matrix reduces the elasticity of the polymer chains resulting in more rigid composites [19–21].

The reinforcing index ( $RI$ ) is an empirical parameter representing a reinforcing effect and can be calculated from the mechanical properties according to the following equation:

$$RI = \{N / [N_0 \cdot (\text{filler content \%} / 100)]\} \quad (6)$$

**T a b l e 4.** The value of reinforcing index ( $RI$ ) for aluminum and cerium sulfate powders

Filler content, phr	$RI$ , %
Aluminum powder	
0	–
10	22.18
20	13.04
30	9.56
40	8.85
50	9.39
60	6.31
Cerium sulfate powder	
10	9.50
20	8.98
30	6.91
40	7.64
50	6.43
60	4.54

where:  $N$  and  $N_0$  are nominal values obtained from the mechanical measurements of the sample, with or without filler, respectively. The calculated  $RI$  values are given in Table 4. The data indicated that the efficiency of powdered aluminum metal (Al) as filler is more than that of Ce(SO<sub>4</sub>)<sub>2</sub> since the  $RI$  of Al is greater than the  $RI$  of Ce(SO<sub>4</sub>)<sub>2</sub>. The obtained data was confirmed by published results [22, 23].

### Thermal analysis

Thermogravimetric analysis (TGA) is one of the most accepted methods for studying the thermal properties of polymer composites. TGA curves provide information about the thermal stability and extent of degradation of the polymeric material. The data obtained from TGA for SBR composites in the absence and presence of 40 phr of aluminum and cerium sulfate powder, respectively, are shown in Fig. 4 and summarized in Table 5. The thermal stability of SBR increases with loading of the investigated fillers and also the decomposition temperature of the SBR/aluminum and SBR/cerium sulfate powder become higher than SBR. This can be attributed to a decrease in the diffusion of volatile gases in the polymer/filler matrix due to the homogeneous distribution of the filler [24, 25]. The thermal stability of the filled samples is higher, at temperatures  $T \geq 500$  °C, *i.e.* after the decomposition of SBR.

**T a b l e 5.** Thermogravimetric data for SBR and SBR/filler composites

Sample	Initial thermal decomposition temperature ( $T_i$ ), °C	Final thermal decomposition temperature ( $T_F$ ), °C	Residual mass, %
SBR	144.50	454.81	5.00
SBR/Al	190.38	598.45	27.37
SBR/CeSO <sub>4</sub>	177.41	657.00	13.72

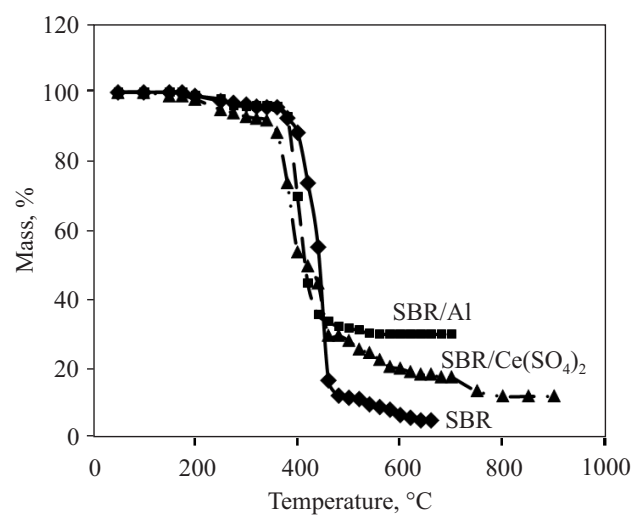


**Fig. 3.** Thermogravimetric analysis of SBR/investigated filler composites

## Electrical properties

To perform a dielectric measurement, the sample is placed between two metallic electrodes, which form a capacitor.

The permittivity  $\epsilon'$ , measures the capacitance whereas dielectric loss,  $\epsilon''$ , measures conductance. These terms were calculated with the contribution of the following equation [26]:

$$\epsilon' = \frac{cd}{A\epsilon_0} \quad (7)$$

$$\epsilon'' = \epsilon' \tan \theta \quad (8)$$

where:  $c$  — the measured capacitance,  $\epsilon_0$  — the permittivity of space,  $\theta$  — the phase angle,  $A$  — the surface area and  $d$  — its thickness.

The effect of concentration of conducting Al, and frequency on the permittivity of SBR/Al composites, are shown in Fig. 4. It is noted that permittivity  $\epsilon'$  increased with higher Al content while it decreased at higher applied frequencies. The increase in  $\epsilon'$  may be due to interfacial polarization arising in electrically heterogeneous materials like composites due to a difference in the conductivity of input raw materials, namely rubber and Al powder [26]. As the Al content increases, the interfacial polarization and formation of a network of conducting Al particles increases in the composites and this could be the reason for an increase of  $\epsilon'$ .

The dielectric loss ( $\epsilon''$ ), as a function of frequency, of SBR/Al composites with different Al content is shown in Fig 4b. It is noted that the specimens filled with Al always showed greater losses than the pure SBR in the whole frequency range. Figure 4b also shows that the

dielectric loss with frequency follows two steps. The first and second regions lie in the frequency range  $10-10^4$  and  $10^4-10^7$  Hz, respectively. A gradual decrease in dielectric loss was noted in the first region, followed by a marginal increase in dielectric loss values in the second region.

Concerning dielectric losses ( $\epsilon''$ ) as a function of frequency, data in the low frequency range depict a relaxation process that must be attributed to an interfacial polarization known as Maxwell-Wagner-Sillar (MWS). This phenomenon appears in heterogeneous media, which consists of phases with different dielectric permittivities and conductivities and is due to the accumulation of charges at interfaces [21]. The molecules present in the unfilled composites are nonpolar in nature and the relaxation is not due to dipole orientation. Hence, a very low dissipation factor and, consequently, very low dielectric losses are noted in unfilled composites [19]. In the filled specimens, there exists one or more interfaces between the filler and the elastomer. Increases in filler content shifts the relaxation peaks to higher frequencies with a simultaneous increase in their abscissa. Heterogeneity is greater in the filled specimens and the MWS effect arising from the filler-polymer interface is superimposed on that of the elastomer [21]. As frequency is increased, the dielectric properties increase considerably.

When the frequency of the applied field is increased, the bound charges (dipoles) present in the composite cannot reorient themselves quickly enough to respond to the applied electric field and, as a result, the dielectric constant decreases. Furthermore, at higher frequencies, the polarizability (electric, ionic and orientation polarization) and electric displacement of dielectric materials

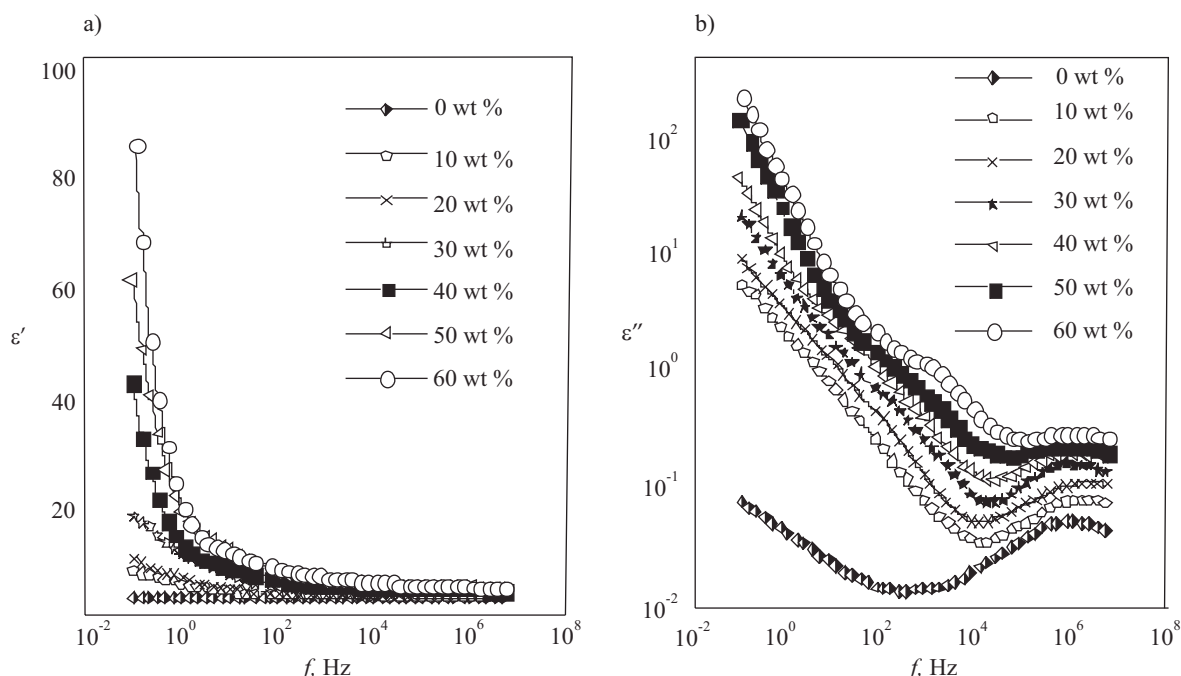


Fig. 4. a) Permittivity ( $\epsilon'$ ), b) dielectric loss ( $\epsilon''$ ) versus applied frequency with various Al contents

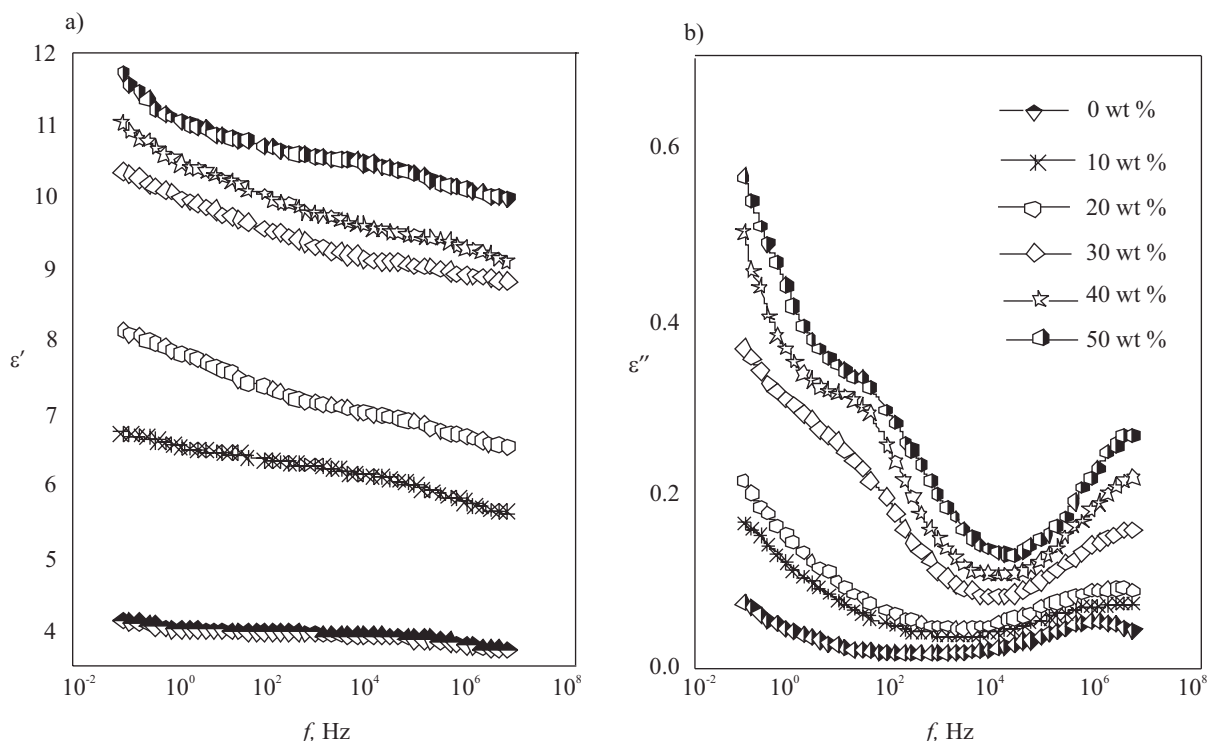


Fig. 5. a) Permittivity ( $\epsilon'$ ) and b) dielectric loss ( $\epsilon''$ ) versus applied frequency with various cerium sulfate contents

were not maintained with the vibration electromagnetic field [27]. For  $\text{Ce}(\text{SO}_4)_2$  filler, (Fig. 5) it appears that both the magnitude of permittivity and dielectric loss decrease at higher frequencies and a slight deviation from linear behavior. From these figures it was noted the increasing ( $\epsilon'$ ) and ( $\epsilon''$ ) values with the increasing of  $\text{Ce}(\text{SO}_4)_2$  content at different frequencies. On the other hand, the dielectric property results showed an improvement, as well as mechanical properties, especially with the addition of Al filler. Such fillers enhance the viscoelastic response to deformation and increase the electrical conductivity and dielectric constant [28].

## CONCLUSIONS

From the above study, it could be concluded that:

- The incorporation of aluminum metallic powder slightly reduces the scorch and cure times of SBR composites, while cure times are increased for SBR/cerium sulfate composites.

- The torque difference  $\Delta M$  increases with higher filler content for aluminum filler due to the increment in crosslink density.

- The tensile strength,  $S_{e100}$  and hardness increased at higher filler content in the SBR matrix, while the elongation at break decreased.

- The swelling percentage decreases with higher aluminum powder and cerium sulfate powder content in SBR composite.

- The experimental results indicate that the dielectric constant and dielectric loss are increased in SBR/Al and SBR/ $\text{Ce}(\text{SO}_4)_2$  composites.

- The dielectric constant decreases at higher frequencies, which can be attributed to the orientation polarization.

## REFERENCES

- [1] Mishra S., Shimpi N.G., Patil U.D.: *J. Polym. Res.* **2007**, *14*, 449. <http://dx.doi.org/10.1007/s10965-007-9127-5>
- [2] Vinod V.S., Varghese S., Kuriakose B.: *J. Appl. Polym. Sci.* **2004**, *91*, 3156. <http://dx.doi.org/10.1002/app.13472>
- [3] Li M., Shi Z., Liu Z. et al.: *J. Rare Earths* **2007**, *25*, 138.
- [4] Anuar J., Mariatti M., Ismail H.: *Polym. Plast. Technol. Eng.* **2007**, *46*, 667. <http://dx.doi.org/10.1080/15583720701271484>
- [5] Wang Q., Yang F., Yang Q., et al.: *Mater. Des.* **2010**, *31*, 1023. <http://dx.doi.org/10.1016/j.matdes.2009.07.038>
- [6] Vinod V.S., Varghese S., Kuriakose B.: *Polym. Degrad. Stab.* **2002**, *75*, 405. [http://dx.doi.org/10.1016/S0141-3910\(01\)00228-2](http://dx.doi.org/10.1016/S0141-3910(01)00228-2)
- [7] Zhang G.Q., Zhou M.H., Ma J.H. et al.: *J. Appl. Polym. Sci.* **2003**, *90*, 2241. <http://dx.doi.org/10.1002/app.12888>
- [8] Marzocca A.J.: *Eur. Polym. J.* **2007**, *43*, 2682. <http://dx.doi.org/10.1016/j.eurpolymj.2007.02.034>
- [9] Shah V.: "Handbook of Plastic Testing Technology", Wiley, USA 1998.
- [10] Mohamed N., Muchtar A., Ghazali M. et al.: *Eur. J. Sci. Res.* **2008**, *24*, 538.
- [11] Varghese S., Karger K.J., Gatos K.G.: *Polymer* **2003**, *44*, 3977. [http://dx.doi.org/10.1016/S0032-3861\(03\)00358-6](http://dx.doi.org/10.1016/S0032-3861(03)00358-6)
- [12] Ciprari D.L.: "Master Thesis", Georgia Institute of Technology 2004.
- [13] Teh P.L., Mohd I.shak Z.A., Hashim A.S. et al.: *Eur. Polym. J.* **2004**, *40*, 2513. <http://dx.doi.org/10.1016/j.eurpolymj.2004.06.025>

- [14] Balachandran A.N., Kurian P., Joseph R.: *Mater. Des.* **2012**, 40, 80. <http://dx.doi.org/10.1016/j.matdes.2012.03.032>
- [15] El-Sabbagh S.H., Ahmed N.M., Selim M.M.: *Pigment Resin Technol.* **2006**, 35, 119. <http://dx.doi.org/10.1108/03699420610665148>
- [16] Lee B.L.: *Rubber Chem. Technol.* **1979**, 52, 1019. <http://dx.doi.org/10.5254/1.3535250>
- [17] Wolf S., Wang M.J.: *Rubber Chem. Technol.* **1992**, 65, 329. <http://dx.doi.org/10.5254/1.3538615>
- [18] Wolf S.: *Rubber Chem. Technol.* **1996**, 69, 325. <http://dx.doi.org/10.5254/1.3538376>
- [19] Al-Ghamdi A.A., El-Tantawy F., Abdel Aal N. et al.: *Polym. Degrad. Stab.* **2009**, 94, 980. <http://dx.doi.org/10.1016/j.polymdegradstab.2009.02.012>
- [20] Vinod V.S., Varghese S., Kuriakose B. et al.: *Kautsch. Gummi Kunstst.* **2002**, 55, 512.
- [21] Siddaramaiah N.M.R., Sudhakar R.D.: *J. Mater. Sci. Mater. Electron.* **2007**, 18, 635. <http://dx.doi.org/10.1007/s10854-006-9077-4>
- [22] Hassan H.H., Ateia E., Darwish N.A. et al.: *Mater. Des.* **2012**, 34, 533. <http://dx.doi.org/10.1016/j.matdes.2011.05.005>
- [23] Helaly F.M., El Sabbagh S.H., El Kinawy O.S. et al.: *Mater. Des.* **2011**, 32, 2835. <http://dx.doi.org/10.1016/j.matdes.2010.12.038>
- [24] Ahmed N.M., El-Sabbagh S.H.: *Mater. Des.* **2011**, 32, 303. <http://dx.doi.org/10.1016/j.matdes.2010.05.039>
- [25] Amraee I.A., Katbab A.A., Aghafarajollah S.H.: *Rubber Chem. Technol.* **1995**, 69, 130. <http://dx.doi.org/10.5254/1.3538353>
- [26] Khalaf A.I., Yehia A.A., Ismail M.N., El-Sabbagh S.H.: *Kautsch. Gummi Kunstst.* **2013**, 9, 28.
- [27] Siddaramaiah N.M.R., Samuel R.D.S., Rajan J.S. et al.: *J. Mater. Sci. Mater. Electron.* **2009**, 20, 648. <http://dx.doi.org/10.1007/s10854-008-9780-4>
- [28] Gunasekaran S., Natarajan R.K., Kala A. et al.: *Indian J. Pure Appl. Phys.* **2008**, 46, 733.

Received 20 I 2014.

## W kolejnym zeszycie ukażą się m.in. następujące artykuły:

- M. Śmiga-Matuszowicz, A. Korytkowska-Wałach, J. Łukaszczyk — Układy polimerowe formowane *in situ* do zastosowań biomedycznych. Cz. I. Implanty wstrzykiwalne
- M. Kędzierski, Z. Bończa-Tomaszewski, G. Jaworska, A. Niska — Warstwowe podwójne wodorotlenki jako katalizatory transestryfikacji i nanonapełniacze żywicy poliestrowej (*j. ang.*)
- R. Oliwa, M. Heneczkowski, M. Oleksy — Kompozyty epoksydowe do zastosowań w przemyśle lotniczym
- B. Grabowska, B. Pilch-Pitera, K. Kaczmarśka, B. Trzebicka, B. Mendrek, D. Drożyński, P. Łątka — Właściwości kompozycji poli(kwas akrylowy)/modyfikowana skrobia stosowanej jako nowe spoiwo polimerowe
- A. Smejda-Krzewicka, W.M. Rzymski, D. Kowalski — Sieciowanie kauczuku chloroprenowego tlenkiem cyny
- W.S. Tan, J.Z. Zhou, S. Huang, W.L. Zhu, X.K. Meng — Wytwarzanie mikroelementów polimerowych z zastosowaniem techniki topienia laserem CO<sub>2</sub> (*j. ang.*)
- K.J. Wilczyński, A. Nastaj — Modelowanie procesu wytłaczania jednoślimakowego z dozowanym zasilaniem mieszanin tworzyw termoplastycznych
- M. Muniesa, Á. Fernández, I. Clavería, C. Javierre, J.A. Sarasua, M. Blanco — Nowa głowica wytłaczarki z wbudowanym urządzeniem ultradźwiękowym i układem bezpośredniego pomiaru parametrów procesu — projekt i testowanie (*j. ang.*)